Thermodynamic and Surface Properties of Sr–Si Liquid Alloy at Different Temperatures

Upendra Mehta, Ramesh Kumar Gohivar, Shashit Kumar Yadav*

Department of Physics, Mahendra Morang Adarsh Multiple Campus Biratnagar, Nepal.

*Corresponding author. Email: sashit.yadav@mmamc.tu.edu.np

Abstract

Thermodynamic and surface properties of Sr–Si liquid alloy have been estimated and explained at different temperatures using quasi–lattice model and Butler's model respectively. The interaction energy parameters, also called model parameters have been determined using the available literature data for excess Gibbs free energy of mixing. The reliability of the model parameters has been obtained by comparing the results of present work with the values of thermodynamic functions calculated using literature data. The mixing behaviour of the system have been analysed by reproducing the thermodynamic, structural and surface properties of the system at 1080 K using optimised model parameters. The temperature dependence of model parameters have been then calculated by assuming their temperature derivative terms to be constant for small change in temperature of the system.

Keywords

Sr–Si liquid alloy, interaction energy, phase transition, surface concentration, surface tension.

1 Introduction

The phase diagram of Sr–Si system along with the details of literature review related to the presence of different stable phases, thermodynamics properties and structural stability of intermetallic compound till 1989 have been summarized by Itkin and Alcock [1]. Palenzona and Pani in 2004 [2] used four different techniques, such as differential thermal analysis (DTA), metallographic analysis, electron microscopy and X-ray diffraction to study the phase diagram of the alloy in the composition range $0 - 75$ at. % Si. They investigated the existence of Sr_2Si, Sr_5Si_3, $SrSi$, $SrSi_2$ intermetallic compounds. Further, their results predicted the occurrence of four eutectics in the system at about

3 at.% Si and 1018 K, 44 at.% Si and 1383 K, 61 at.% Si and 1328 K, and 74 at.% Si and 1318 K [2]. Later, Balducci et al. in 2005 [3] reinvestigated the existence of different phases in the strontium silicides reported by Palenzona and Pani [2]. For the purpose, they used the Knudsen Effusion Mass Spectrometry and Knudsen Effusion Weight Loss techniques in the temperature range 665–1300 K. They also measured the enthalpies of formation for Sr_2Si to be -39.7 ± 3.2 kJ/mol, Sr_5Si_3 to be -43.8 ± 3.6 kJ/mol, $SrSi$ to be -51.7 ± 4.1 kJ/mol and $SrSi_2$ to be -40.3 ± 3.7 kJ/mol at 298 K.

Meanwhile, Garay et al. in 2009 [4] used computer-

based software CALPHAD for the thermodynamic modeling of Si–Sr system. In due course, they considered the stoichiometric intermetallic compounds of the types Sr_2Si, Sr_5Si_3 and $SrSi$, and non-stoichiometric phase as $SrSi_2$. They modeled the liquid phases of the system using ramdom solution model and assiciated solution model, and presented the self-consistent parameters for excess Gibbs free energy of mixing in the framework of Redlich-Kister (R-K) polynomial. The microhardness and instrumental neutron activation analysis experimental methods were used by Rygalin et al. [5] to measure the solid solubilities of Sr and Ba impurity gatters in Si in the range 1173–1573 K. The Si-rich composition range of phase diagrams of Si–Sr and Si–Ba were investigated by them for the first time. Their measurements showed that the solubility of Sr and Ba in Si were 1.15 at. % and 0.98 at. % respectively at 1573 K.

Li et al. in 2011 [6] thermodynamically reassessed the system considering the experimental phase diagram data of Rygalin et al. [5]. Moreover, they used substitutional solution and associated models to obtain the self-consistent thermodynamic parameters for the liquid phase of the system. Their results found to be consistent with the experimental measurements. Recently, Yi et al. [7] critically analysed the available experimetal data on thermodynamic properties and phase equilibria of binary Si–Sr and ternary Al–Si–Sr alloys. On these fundamentals, they used CALPHAD technique to update the thermodynamic description of the systems. Their results for Si–Sr were found to be in better agreement with the experimental data in compared to the prevailing assessments.

Therefore, the self-consistent parameters for excess Gibbs free energy of mixing presented by Yi et al. [7] have been used in present work to calculate and explain the temperature and concentration-dependent thermodynamic and surface properties of Sr–Si liquid alloy. Quasi-lattice model [8–12] have been used to calculate the thermodynamic and structural properties of the system at 1080 K assuming the existence of intermetallic stable compound of type Sr_2Si [1,4,7]. The reliability of model parameters have been analysed by comparing the calculated results with the available literature data. Then after, the model parameters have been estimated at different temperatures, with the aid of which thermodynamic and surface properties (using Butler's model [13–16]) of the system have been computed in the temperature range 1080–1380 K.

2   Theory

2.1   Quasi–lattice model

Following quasi–lattice model, the expression for excess Gibbs free energy of mixing (ΔG_M^{xs}) for the binary complex of the type A_2B (equivalent to Sr_2Si) can be given as [8–11]

$$\Delta G_M^{xs} = N[\Phi\Delta\omega + \Phi_{AB}\Delta\omega_{AB} + \Phi_{AA}\Delta\omega_{AA}] \quad (1)$$

Herein, $\Delta\omega$, $\Delta\omega_{AB}$ and $\Delta\omega_{AA}$ are the model parameters which need to be determined. They are assumed to be depend linearly on temperature but are concentration independent. Moreover, Φ, Φ_{AB} and Φ_{AA} are the simple polynomials in x_1 and $x_2 = 1 - x_1$, are given by the following relations

$$\Phi = x_1(1 - x_1)$$
$$\Phi_{AB} = \frac{x_1}{6} + x_1^2 - \frac{5x_1^3}{3} + \frac{x_1^4}{2}$$
$$\Phi_{AA} = -\frac{x_1}{4} + \frac{x_1^2}{2} - \frac{x_1^4}{4} \quad (2)$$

The enthalpy of mixing (ΔH_M) can be expressed in terms of ΔG_M^{xs} by the standard thermodynamic relation as

$$\Delta H_M = \Delta G_M^{xs} - T\left(\frac{\partial\Delta G_M^{xs}}{\partial T}\right)_P \quad (3)$$

Using Equation (1) in the above, one can obtain

$$\Delta H_M = \Delta G_M^{xs} - TN\left[\frac{\partial\Delta\omega}{\partial T}\Phi + \frac{\partial\Delta\omega_{AB}}{\partial T}\Phi_{AB} + \frac{\partial\Delta\omega_{AA}}{\partial T}\Phi_{AA}\right] \quad (4)$$

Herein, $\frac{\partial\Delta\omega}{\partial T}$, $\frac{\partial\Delta\omega_{AB}}{\partial T}$ and $\frac{\partial\Delta\omega_{AA}}{\partial T}\Phi_{AA}$ are the temperature derivative terms of interaction energy parameters.

The activity of component i $(a_i; i = Er, Al)$ in the binary solution can be expressed in terms of ΔG_M as

$$RT\ln a_i = \Delta G_M + (1 - x_i)\left(\frac{\partial\Delta G_M}{\partial x_i}\right)_{T,P,N} \quad (5)$$

Using Equations (1) in Equation (5), one can obtain the expression for $\left(\frac{\partial\Delta G_M}{\partial x_i}\right)_{T,P,N}$ as

$$\left(\frac{\partial\Delta G_M}{\partial x_i}\right)_{T,P,N} = \Delta\omega\Phi' + \Delta\omega_{AB}\Phi_{AB}'$$
$$+ \Delta\omega_{AA}\Phi_{AA}' + \ln\left(\frac{x_i}{1 - x_i}\right) \quad (6)$$

where Φ' and Φ'_{ij} are the first order derivatives of respective parameters (in Equation (2)) with respect to concentration of ith element.

ΔG_M^{xs} can be expressed in terms of Gibbs free energy of mixing (ΔG_M) as

$$\Delta G_M = \Delta G_M^{xs} + RT[x_1 \ln x_1 + x_2 \ln x_2] \qquad (7)$$

where R is the real gas constant and T is the absolute temperature.

The expression for concentration fluctuation in long wavelength limit ($S_{CC}(0)$) is expressed as [9, 10, 16]

$$S_{CC}(0) = RT \left(\frac{\partial^2 G_M}{\partial x_1^2} \right)^{-1}_{T,P,N}$$
$$= RT \left(\frac{\partial^2 G_M}{\partial x_2^2} \right)^{-1}_{T,P,N} \qquad (8)$$

Using Equations (1) and (7) in Equation (8) one can obtain

$$S_{CC}(0) = x_1 x_2 [1 + x_1 x_2 RT(\Delta\omega\Phi'' + \Delta\omega_{AB}\Phi''_{AB}$$
$$+ \Delta\omega_{AA}\Phi''_{AA})]^{-1} \qquad (9)$$

where Phi'' and Phi_{ij}'' are the second order derivatives of thye terms in Equation (2) with respect to concentration (x_i). The ideal values of $S_{CC}(0)$ is obtained by the following relation

$$S_{CC}^{id}(0) = x_1 x_2 \qquad (10)$$

The structural functions, Warren-Cowley short range–order parameter (α_1) and the ratio of mutual to intrinsic diffusion coefficients (D_M/D_{id}) can be expressed in terms of $S_{CC}(0)$ as [9, 16, 17]

$$\alpha_1 = \frac{S-1}{[S(Z-1)+1]} \qquad (11)$$

where

$$S = \frac{S_{CC}(0)}{S_{CC}^{id}(0)} \qquad (12)$$

2.2 Butler's model

According to this model, the surface tension (σ) of the binary liquid alloy can be given as [9, 13–16]

$$\sigma = \sigma_1^0 + \frac{RT}{A_1} \ln \left(\frac{x_1^s}{x_1} \right) + \frac{\Delta G_{s,1}^{xs} - \Delta G_{b,1}^{xs}}{A_1}$$
$$= \sigma_2^0 + \frac{RT}{A_2} \ln \left(\frac{x_2^s}{x_2} \right) + \frac{\Delta G_{s,2}^{xs} - \Delta G_{b,2}^{xs}}{A_2} \qquad (13)$$

where σ_i^0 is the surface tension of the pure atom, A_i is the molar surface area of pure atom, x_i^s is the surface concentration of pure atom, and $\Delta G_{i,s}^{xs}$ and $\Delta G_{i,b}^{xs}$ are the partial excess Gibbs free energy of pure component in the binary liquid mixture. The relation between $\Delta G_{i,s}^{xs}$ and $\Delta G_{i,b}^{xs}$ can be given as

$$\Delta G_{s,i}^{xs} = \beta \Delta G_{b,i}^{xs} \qquad (14)$$

where β is the coordination number of individual atom in the surface phase and bulk phase. The appropriate value of β is taken to be 0.8181 by [9, 15] for the simple liquid element.

The surface tension ($\sigma_i^0(T)$) and density ($\rho_i(T)$) of pure elements at temperature T are obtained in terms of surface tension ($\sigma_i^0(T_0)$) and density ($\rho_i(T_0)$) near their melting temperature T_0 are expressed using the linear equations

$$\sigma_i^0(\mathrm{T}) = \sigma_i^0(\mathrm{T}_0) + \frac{\partial \sigma_i^0}{\partial T}(T - T_0),$$
$$\rho_i(T) = \rho_i(T_0) + \frac{\partial \rho_i}{\partial T}(T - T_0) \qquad (15)$$

where $\partial \sigma_i^0/\partial T$ and $\partial \rho_i/\partial T$ are the temperature derivative of surface tension and density of the individual components in their pure state respectively.

2.3 Redlich-Kister (R-K) polynomial

In this frame, ΔG_M^{xs} is expressed as [?, 18, 19]

$$\Delta G_M^{xs} = x_1 x_2 \sum_{k=0}^{n} L_k (x_1 - x_2)^k \qquad (16)$$

where L_k are the linear T–dependent coefficients or interaction energy parameters of R-K polynomial. They are expressed in the form $L_k = a_k + b_k T$, where a_k (in J/mol) are ΔH_M contributed terms and b_k (in J/mol-K) are ΔS_M^{xs} contributed terms. The partial excess Gibbs free energy (ΔG_i^{xs}) of the component i in the binary liquid alloy can be given as [12, 19]

$$\Delta G_i^{xs} = \Delta G_M^{xs} + (1 - x_i) \left(\frac{\partial \Delta G_M^{xs}}{\partial x_i} - \frac{\partial \Delta G_M^{xs}}{\partial (1 - x_i)} \right)$$
$$\qquad (17)$$

The activity coefficient of component i in the binary solution is related to ΔG_i^{xs} as

$$RT \ln \gamma_i = \Delta G_i^{xs} \qquad (18)$$

After the computations of γ_i, the activity of component i can be obtained by the relation

$$a_i = x_i \gamma_i \qquad (19)$$

Using Equations (9) and (16), $S_{CC}(0)$ for this system having $k = 0, 1, 2$ can be obtained as [9, 19]

$$S_{CC}(0) = RT[-2L_0 + (-12x_1 + 6)L_1$$
$$+(-48x_1^2 + 48x_1 - 10)L_2 + \frac{RT}{x_1(1-x_1)}]^{-1} \qquad (20)$$

The values of other structural functions in this frame work can also be obtained using Equations (10-12).

3 Results and Discussion

3.1 Thermodynamic and structural properties

From the knowledge gained from literature review, the authors of present work reveals that only a few of thermodynamic properties of Sr–Si liquid alloy is available to date. In this regard, the self-consistent parameters for the excess Gibbs free energy of mixing (ΔG_M^{xs}) presented by Yi et al. [7] (Table 1) have been considered as reference to optimise the model parameters. The values of ΔG_M^{xs} have been calculated at 1080 K using Equation (16) with the aid of parameters from Table 1. Considering them as reference values, the best fit values of model parameters have been determined using Equations (1) and (2) and are tabulated in Table 1. The calculated values of ΔG_M^{xs} have been compared with the available literature data in Figure 1.

Table 1: Self-consistent parameters for ΔG_M^{xs} of Sr–Si liquid alloy

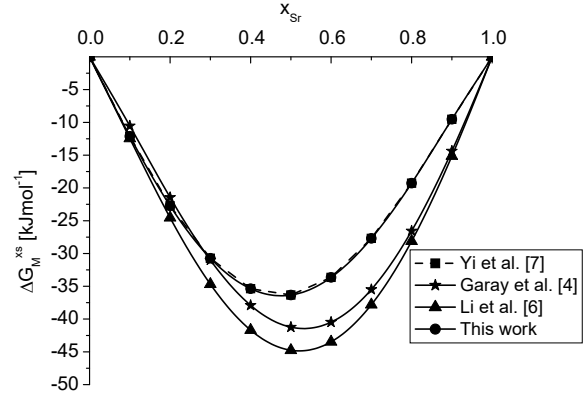| Parameters [J/mol]	Reference
$L_{Sr,Si}^0 = -180478 + 14.367 * T$ $L_{Sr,Si}^1 = -11506 - 14.061 * T$ $L_{Sr,Si}^2 = 6671 + 31.293 * T$	[4]
$L_{Si,Sr}^0 = -179060.0$ $L_{Si,Sr}^1 = -43906.0 + 23.40921 * T$ $L_{Si,Sr}^2 = 40325.2$	[6]
$L_{Si,Sr}^0 = -184417.0 + 36.182 * T$ $L_{Si,Sr}^1 = -12874.7 - 4.768 * T$ $L_{Si,Sr}^2 = 39167.2$	[7]
$\Delta\omega = -22986.5 + 32.09204 * dT$ $\Delta\omega_{AB} = -166373 + 7.4826 * dT$ $\Delta\omega_{AA} = 293928 + 8.48028 * dT$	This work

Figure 1: The calculated values of ΔG_M^{xs} versus x_{Sr} for Sr–Si liquid alloy at 1080 K.

It can be observed that calculated values of ΔG_M^{xs} at 1080 K using the parameters of present work are in excellent agreement with those of Yi et al. [7] at all concentrations, Figure 1. They are also found to be in good agreement with the values computed using parameters of Garay et al. [4] in the concentration range $x_{Sr} \leq 0.3$ and those of Li et al. [6] in ($x_{Sr} < 0.2$). The maximum negative value of ΔG_M^{xs} are found to be -36.3351 kJ/mol [7] and -36.3351 kJ/mol (this work) at $x_{Sr} = 0.5$ and 1080 K. Thus, the model parameters obtained in the present work have been preferred for further calculations of other thermodynamic, structural and surface properties of the system. Moreover, the system is found to be symmetric with respect to ΔG_M^{xs} and strong interacting in nature at/about equi-atomic compositions.

The activities of components Sr (a_{Sr}) and Si(a_{Si}) in Sr–Si liquid alloy have been calculated using Equations (5) and (6) with the help of model parameters in Table 1. Likewise, the reference values as well as other literature values of a_{Sr} and a_{Si} have been calculated using Equations (17-19) and parameters from Table 1. The compositional variation of a_{Sr} and a_{Si} at 1080 K is plotted in Figure 2.

From Figure 2, it is found that the calculated values of a_{Sr} and a_{Si} using the optimised parameters of this work and Yi et al. [7] are in excellent agreement with each other at all compositions. However, they deviate from the values estimated using parameters of Garay et al. [4] and Li et al. [6]. Moreover, the determined values of a_{Sr} and a_{Si} show strong negative deviation from ideal values in the lower and intermediate concentrations of Sr indicating the system to be strong interacting in nature. Meanwhile, they show slight positive deviation from ideal values at higher concentration range $x_{Sr} > 0.85$ conveying the system to be seg-

regating in nature, Figure 2. The results obtained from the investigations of ΔG_M^{xs} and a are similar to each other.
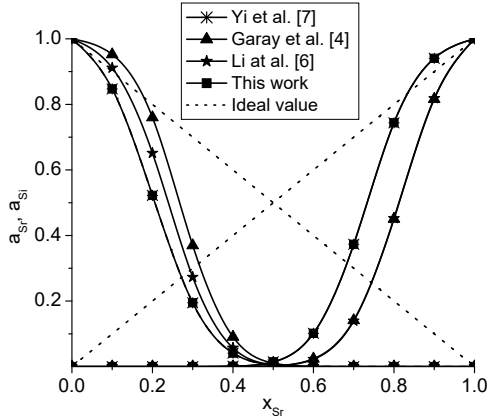

Figure 2: Compositional dependence of a_{Sr} and a_{Si} for Sr–Si liquid alloy at 1080 K.

The reference value for the enthapy of mixing (ΔH_M) of the system has been obtained employing Equation (3) and the input parameters from Table 1. The temperature derivative terms of interaction energy parameters ($\frac{\partial \Delta \omega}{\partial T}$, $\frac{\partial \Delta \omega_{AB}}{\partial T}$ and $\frac{\partial \Delta \omega_{AA}}{\partial T}$) have then been obtained using Equations (3) and (4) and with the help of above determined values of ΔG_M^{xs}. The best fit values of the respective parameters are $\frac{\partial \Delta \omega}{\partial T} = 32.09204$, $\frac{\partial \Delta \omega_{AB}}{\partial T} = 7.4826$ and $\frac{\partial \Delta \omega_{AA}}{\partial T} = 8.48028$. The calculated values of ΔH_M of present work along with those obtained using the parameters of ref. [4, 6, 7] are plotted as a function of x_{Sr} in Figure 3.

The results of the work are in excellent agreement with those obtained from Yi et al. [7] and also in good agreement with those computed using the parameters of ref. [4, 6] at lower range of x_{Sr}. The calculated values of $\Delta H_M = -46.1043$ kJ/mol [7] and $\Delta H_M = -46.1195$ kJ/mol (present work) at $x_{Sr} = 0.5$ and 1080 K, Figure 3. Hence, the system is again found to be symmetric in nature with respect to enthalpy of mixing.
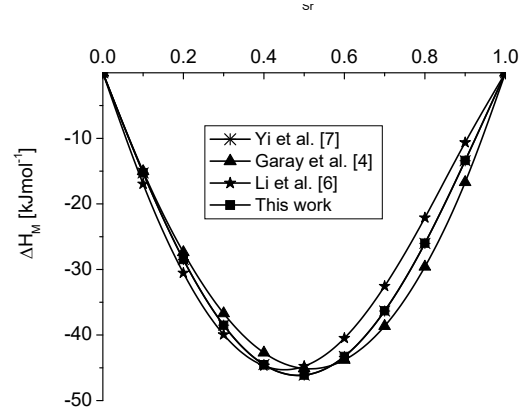

Figure 3: Compositional dependence of ΔH_M for Sr–Si liquid alloy at 1080 K.

To gather further information about the mixing behaviour of the system, the structural properties like concentration fluctuation in long wavelength limit ($S_{CC}(0)$) and Warren-Cowley short-range order parameter (α_1) [9, 10, 17] have been calculated. The values of these structural functions have been computed using Equations (8-12) and the parameters in Table 1. The values of these functions have also been computed using the parameters of Yi et al. [7] and Equation (20). The computational dependence of values so obtained are plotted in Figure 4.
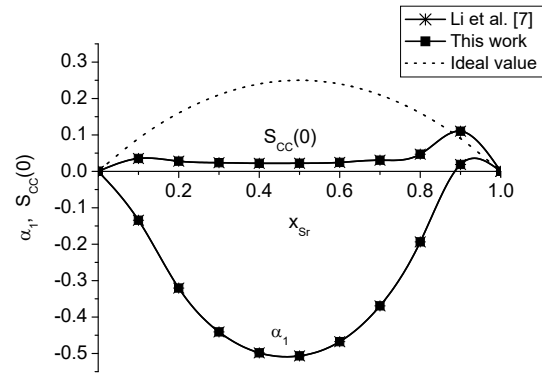

Figure 4: Compositional dependence of $S_{CC}(0)$ and α_1 for Sr–Si liquid alloy at 1080 K.

For a specific temperature and concentration, if $S_{CC}(0) < S_{CC}^{id}(0)$ and $\alpha_1 < 0$, then hetero-coordinating tendency in the liquid alloy is expected and if $S_{CC}(0) > S_{CC}^{id}(0)$ and $\alpha_1 > 0$, then homo-coordinating tendency is expected. The former is also called ordering nature whereas the later is called segregating nature. Under similar conditions, if $\alpha_1 = 0$, then ideal mixing tendency in the alloy is expected [9, 12]. The perusal of Figure 4 shows that the estimated values of $S_{CC}(0) < S_{CC}^{id}(0)$

and $\alpha_1 < 0$ in the concentration range $x_{Sr} < 0.85$ indicating the ordering nature of the system. Meanwhile, $S_{CC}(0) > S_{CC}^{id}(0)$ and $\alpha_1 > 0$ at $x_{Sr} > 0.85$ corresponding the segregating tendency in the liquid alloy. These results are in accordance with those revealed by the investigations of thermodynamic functions.

In order to analyse the mixing behaviours of the system at higher temperatures, the thermodynamic properties (ΔG_M^{xs} and a) have been estimated in the range 1080–1380 K. For the purpose, the model parameters ($\Delta\omega$, $\Delta\omega_{AB}$ and $\Delta\omega_{AA}$) are assumed to depend linearly on temperature. Temperature dependence of these parameters in terms of $\partial\Delta\omega/\partial T$, $\partial\Delta\omega_{AB}/\partial T$ and $\partial\Delta\omega_{AA}/\partial T$ can be expressed as [12, 16]

$$\Delta\omega(T) = \Delta\omega(T_0) + \frac{\partial\Delta\omega}{\partial T}(T - T_0)$$

$$\Delta\omega_{ij}(T) = \Delta\omega_{ij}(T_0) + \frac{\partial\Delta\omega_{ij}}{\partial T}(T - T_0) \qquad (21)$$

Herein, T_0 (=1080 K) is the melting temperature of the system and T is the temperature of interest. The variations of above mentioned model parameters as a function of temperature are presented in Table 1.
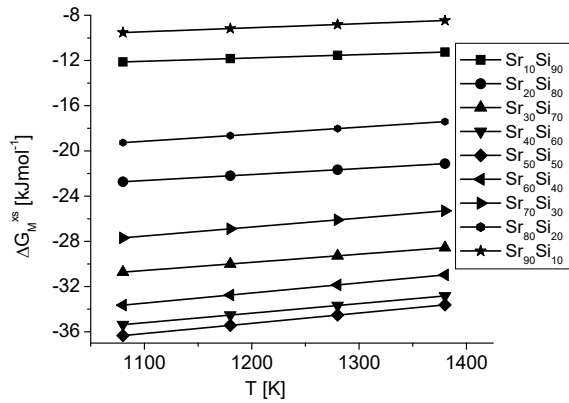

Figure 5: Variation of ΔG_M^{xs} with temperature for Sr–Si liquid alloy.

ΔG_M^{xs} of the system have been computed in the temperature range 1080-1380 K using Equations (1 and 2) and parameters from Table 1. Likewise, the values of a_{Sr} and a_{Si} have been computed using Equations (5 and 6). The obtained values of ΔG_M^{xs} and a_{Sr} and a_{Si} at different temperatures are plotted in Figures 5 and 6 respectively.

The negative value of ΔG_M^{xs} gradually and linearly decreases with increase in temperature of the system, Figure 5. At equiatomic composition ($Sr_{50}Si_{50}$), the determined values of ΔG_M^{xs} are -36.3351 kJ/mol -35.4291 kJ/mol, -34.5231 kJ/mol and -33.6172 kJ/mol at 1080 K, 1180 K, 1280 K and 1380 K respectively. The activities of both the components in the system increase and gradually get close to their respective ideal values with increase in temperature, Figure 6. The estimated values of a_{Sr} and a_{Si} at $Sr_{50}Si_{50}$ are (0.0144, 0.0053), (0.0216, 0.0084), (0.0304, 0.0125) and (0.0408, 0.0175) respectively at 1080 K, 1180 K, 1280 K and 1380 K. These results indicate that the ordering or compound forming nature of the alloy gradually declines at higher temperatures. Moreover, the system shows ideal mixing behaviour at higher temperatures.
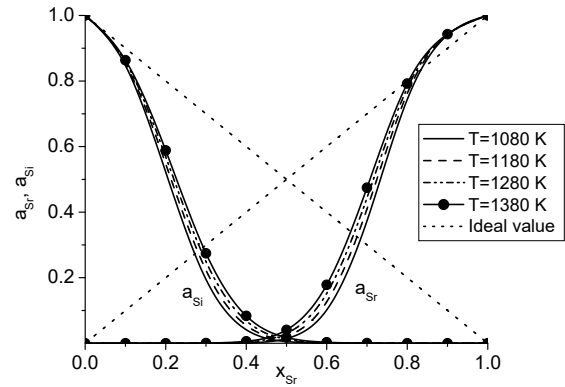

Figure 6: Compositional and temperature dependence of a_{Sr} and a_{Si} for Sr–Si liquid alloy.

3.2 Surface properties

The surface tension (σ) of the liquid alloy and the surface concentrations (x_{Sr}^s and x_{Si}^s) of its components at 1083 K have been calculated using Equations (12-15) and parameters from Table 2. The values so estimated are plotted as a function of concentration of Sr in Figures 7 and 8.

The estimated value of surface tension of Sr (σ_{Sr}) is 0.2993 Nm^{-1} and that of Si (σ_{Si}) is 0.9434 Nm^{-1} at 1080 K. As a result, the calculated value of x_{Sr}^s is found to be greater than its ideal value while that of x_{Si}^s is found to be less than its ideal value at all concentrations, Figure 7. Thus, Sr atoms segregate in the surface phase whereas Si atoms remain in the bulk phase of the liquid mixture. Moreover, the calculated value of surface tension of the liquid alloy is less than its ideal value at all concentrations, Figure 8.

Table 2: Density (ρ_i)[kgm^{-3}] and surface tension (σ_i) [Nm^{-1}] of pure component [20]

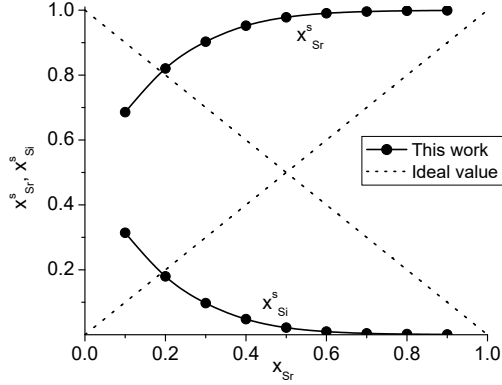| |
|---|
| $\rho_{Sr} = 2370 - 0.26(T - 1043)$ |
| $\rho_{Si} = 2530 - 0.35(T - 1683)$ |
| $\sigma_{Sr} = 0.303 - 1.3 \times 10^{-4}(T - 1043)$ |
| $\sigma_{Si} = 0.865 - 1.0 \times 10^{-4}(T - 1043)$ |

value at higher temperature (Figure 10) conveying the movement of respective atoms from bulk phase to the surface phase.

The surface tension of the liquid alloy gradually and linearly decreases with increase in temperature. This result corresponds that the cohesive energy or interaction between the atoms of liquid mixture gradually decreases. Moreover, the system shows ideal mixing behaviour at higher temperatures.

Figure 7: Variation of x^s_{Sr} and x^s_{Si} with x_{Sr} of Sr–Si liquid alloy at 1080 K.

Figure 9: Compositional and temperature dependence of x^s_{Sr} and x^s_{Si} for Sr–Si liquid alloy.

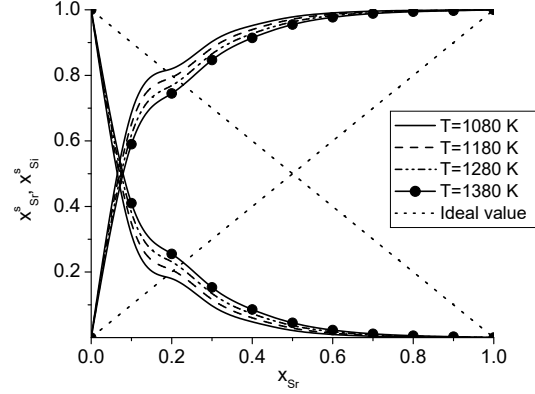Figure 8: Compositional dependence of σ for Sr–Si liquid alloy at 1080 K.
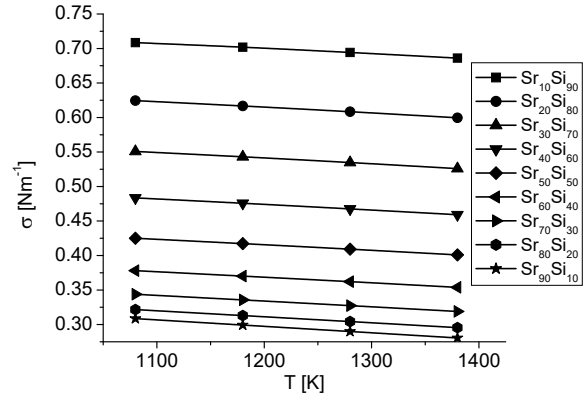
Figure 10: The calculated values of σ for Sr–Si liquid alloy at different temperatures.

The vales of x^s_{Sr}, x^s_{Si} and σ have also been estimated at aforementioned temperatures following the above procedure using the determined values of partial excess Gibbs free energy (ΔG^{xs}_i) of components. It can be observed that the estimated value of x^s_{Sr} gradually decreases and move towards its ideal value with increase in temperature, Figure 9. It indicates the gradual movement of respective atoms from the surface phase to the bulk phase of liquid mixture. Moreover, the calculated value of x^s_{Si} gradually increases and gets close to its ideal

4   Conclusions

The important conclusions of the work are summarized as follows:

- The estimated values of thermodynamic functions of Sr–Si liquid alloy at 1080 K are in well agreement with reference values.

- The model parameters have well explained

the thermodynamic, structural and surface properties of the system.

- The system is found to be strong interacting in nature at lower and intermediate concentrations of Sr whereas it shows demixing tendency at higher concentration range, $x_{Sr} > 0.9$.

- The compound forming strength between the components of liquid mixture gradually decreases with increase in temperature.

- The atoms of Sr segregate in the surface phase whereas those of Si remain in the bulk phase at 1080 K. As the temperature of mixture has been gradually increased, Sr atoms tend to move towards the bulk phase while those of Si tend to move towards the surface phase.

- The surface tension of the liquid alloy gradually and linearly decreases with at elevated temperatures.

References

[1] Itkin VP, Alcock CB. The Si-Sr (Silicon-Strontium) system. Bulletin of Alloy Phase Diagrams. 1989;10(6):630–634.

[2] Palenzona A, Pani M. The phase diagram of the Sr–Si system. Journal of alloys and compounds. 2004;373(1-2):214–219.

[3] Balducci G, Brutti S, Ciccioli A, Gigli G, Trionfetti G, Palenzona A, et al. Vapor pressures and thermodynamic properties of strontium silicides. Intermetallics. 2006;14(5):578–583.

[4] Garay A, Trapaga G, Liu Z, Arroyave R. Thermodynamic modeling of the Si–Sr system. Calphad. 2009;33(3):550–556.

[5] Rygalin B, Prokofieva V, Pavlova L, Sokolov YE. The Si–Sr and Si–Ba phase diagrams over the Si-rich composition range. Calphad. 2010;34(2):196–199.

[6] Li K, Liu S, Sha C, Du Y. A thermodynamic reassessment of the Si–Sr system. Calphad. 2011;35(4):594–600.

[7] Yi W, Gao J, Tang Y, Zhang L. Thermodynamic descriptions of ternary Al–Si–Sr system supported by key experiments. Calphad. 2020;68:101732.

[8] Adhikari D, Yadav SK, Jha LN. Thermophysical properties of Mg-Tl melt. Journal of Basic and Applied Research International. 2015;9:103–110.

[9] Yadav SK. Thermodynamic, structural and surface properties of rare earth metallic alloys: Au-La liquid system. BIBECHANA. 2023;20(3):316–325.

[10] Bhatia AB, Hargrove WH. Concentration fluctuations and thermodynamic properties of some compound forming binary molten systems. Physical Review B. 1974;10(8):3186.

[11] Bhatia AB, Singh RN. A quasi–lattice theory for compound forming molten alloys. Physics and Chemistry of Liquids an International Journal. 1984;13(3):177–190.

[12] Yadav SK. Assessment of Thermodynamic and Structural Properties of Al–Er liquid alloy at Different Temperatures. The Journal of Knowledge and Innovation. 2023;p. 66–74.

[13] Butler JAV. The thermodynamics of the surfaces of solutions. Proceedings of the Royal Society of London Series A, Containing Papers of a Mathematical and Physical Character. 1932;135(827):348–375.

[14] Kaptay G. A unified model for the cohesive enthalpy, critical temperature, surface tension and volume thermal expansion coefficient of liquid metals of bcc, fcc and hcp crystals. Materials Science and Engineering: A. 2008;495(1-2):19–26.

[15] Kaptay G. Improved derivation of the Butler equations for surface tension of solutions. Langmuir. 2019;35(33):10987–10992.

[16] Yadav SK, Gautam M, Adhikari D. Mixing properties of Cu–Mg liquid alloy. AIP Advances. 2020;10(12):125320.

[17] Warren BE. X-ray diffraction, Addition-Wesley. Reading, MA. 1969;p. 264.

[18] Redlich O, Kister AT. Algebraic representation of thermodynamic properties and the classification of solutions. Industrial & Engineering Chemistry. 1948;40(2):345–348.

[19] Gohivar RK, Yadav SK, Koirala RP, Adhikari D. Assessment of thermo-structural properties of Al-Fe and Fe-Si alloys at high temperatures. Physics and Chemistry of Liquids. 2021;59(5):679–689.

[20] Brandes EA, Brook GB. Smithells metals reference book. Elsevier; 2013.